ISSN 1063-7826, Semiconductors, 2024, Vol. 58, No. 5, pp. 464–472. © Pleiades Publishing, Ltd., 2024.
Russian Text © The Author(s), 2023, published in Fizika i Tekhnika Poluprovodnikov, 2023, Vol. 57, No. 8, pp. 684–692.
English Text © Ioffe Institute, 2023.

Analysis of Stability of Generation in Quantum Well Lasers

Z. N. Sokolova[a],* and L. V. Asryan[b],**

[a]*Ioffe Institute, St. Petersburg, 194021 Russia*
[b]*Virginia Polytechnic Institute and State University, Blacksburg, VA 24061, USA*
**e-mail: zina.sokolova@mail.ioffe.ru*
***e-mail: asryan@vt.edu*

Received October 5, 2023; revised November 11, 2023; accepted November 14, 2023

Abstract—A stability analysis of two modes of generation in semiconductor quantum well lasers is performed. These modes correspond to two solutions of the rate equations obtained by taking into account the internal optical loss that depends on the density of charge carriers injected into the laser waveguide region and, hence, on the injection current. It is shown that, in contrast to the first ("conventional") mode of generation, which is always stable and hence observable, the second ("additional") mode, which is entirely due to the internal loss that depends on the carrier density, is unstable and hence cannot be observed under the steady-state conditions in the laser structure considered in this work.

Keywords: semiconductor lasers with low-dimensional active region, internal optical loss, linear analysis of stability

DOI: 10.1134/S1063782624050154

1. INTRODUCTION

Semiconductor injection lasers based on heterostructures emerged more than 50 years ago. They were invented in 1970, when a laser based on an AlGaAs–GaAs heterostructure was pioneered at the A.F. Ioffe Institute of Physics and Technology, operating in continuous wave mode at room temperature [1].

Modern life is almost impossible to imagine without the use of heterostructure lasers. Such lasers have been widely applied, in particular, in information technology, industry, medicine and everyday life. Recently, much attention has also been paid to the development of lidars ("light radars") based on semiconductor lasers for use in unmanned aerial vehicles and underwater vehicles, as well as in cars.

Over the years, heterostructure lasers, especially lasers with a low-dimensional active region, have been the subject of extensive research (see, for example, [2–29]). Back in the 2000s, it was predicted in works [30–33] that in such lasers there should be a decrease in optical power with an increase in pump current (the so-called rollover of the light-current characteristic (LCC) – dependence of the output optical power on the pump current) for the "conventional" (first) mode of generation of stimulated emission and the existence of an "additional" (second) mode of generation is also possible. Both the LCC rollover for the first mode of generation and the very existence of the second mode are entirely due to (i) the non-instantaneous capture of charge carriers from the bulk waveguide region (optical confinement layer (OCL)) of the laser into the low-dimensional active region and (ii) internal optical loss that depends on the carrier concentration in the waveguide region. (There is also internal optical loss in the lowdimensional active region, but it is significantly lower than the loss in the bulk waveguide region). The characteristics of lasers, in particular the LCC, are radically different for the two modes of generation and, thus, are degenerate (have two branches) (Fig. 1).

The criterion for the existence of the second mode of generation (and, accordingly, the second branch in laser characteristics) can be presented in the following form:

$$\frac{\sigma_{\text{int}} v_{\text{capt},0}}{2bB_{\text{3D}}g^{\max}} > 1, \tag{1}$$

where σ_{int}—cross section of internal optical loss in the waveguide region of the laser structure; $v_{\text{capt},0}$—capture velocity of charge carriers from the bulk (three-dimensional) waveguide region into an unfilled low-dimensional active region, which is a single or multiple quantum wells or layer(s) with quantum dots, b—width of the waveguide region; B_{3D}—coefficient of spontaneous radiative recombination in the waveguide region [11, 19, 34]; $g^{\max}$—maximum modal gain coefficient due to stimulated radiative transitions in the low-dimensional active region of the laser [11, 15, 18, 34].

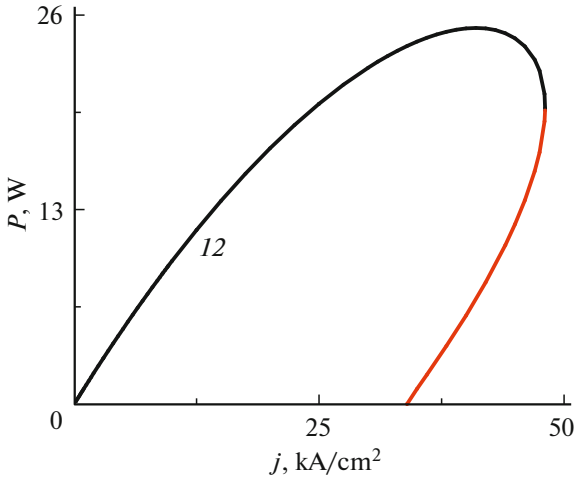

Fig. 1. Steady-state light-current characteristic of a single QW laser with a broadened waveguide and a lasing wavelength of 0.98 μm. *1* – stable first ("conventional") mode of generation, *2* – unstable second ("additional") mode of generation.

The dependence of internal optical loss on the concentration of carriers in the waveguide region is taken into account by the non-zero value of the cross section σ_{int} (in units of cm^2) of internal loss in the waveguide region (see below expression (5) for the coefficient of internal optical loss).

The non-instantaneous capture of carriers from the waveguide region into the low-dimensional active region is taken into account by the finite (not infinitely high) value of the capture velocity $v_{capt,0}$ (in units of cm/s) [34–38] (see below equations (2) and (3)).

The non-instantaneous capture, in combination with spontaneous radiative and (or) Auger recombinations of carriers in the waveguide region, leads to intrinsic sublinearity of the LCC in lasers with a low-dimensional active region [34–38]. However, this non-instantaneousness in itself cannot lead to a LCC rollover. Rollover of LCC does not occur even in a situation where charge carriers are first captured from the waveguide region to the nonemitting upper level of size quantization in the active region, and then relax to the emitting lower (ground) level. In this case, the non-instantaneousness of relaxation, combined with the non-instantaneousness of capture, further enhances the sublinearity of the LCC is the output optical power saturates (asymptotically approaches its maximum possible value) with increasing pump current [39, 40].

Thus, it is the combination of internal optical loss, which depends on the concentration of carriers in the waveguide region, with the non-instantaneousness of capture from the waveguide region that leads to the LCC rollover for the "conventional" (first) mode of generation. And it is the combination of these factors that leads to the emergence of the "additional" (second) mode of generation.

Both the LCC rollover for the conventional mode of generation and the emergence of an additional mode of generation can significantly affect the output optical power and other important characteristics of lasers with a low-dimensional active region. In connection with this, it seems relevant to conduct a detailed study of such lasers, properly taking into account the above factors. In works [30–33, 41–45], as a first step, both modes of generation (in particular, both branches of the LCC) were theoretically studied under steady-state conditions.

The next step, which naturally follows from the first, is a theoretical study of the stability of the two modes of generation, which is the focus of this article in the context of quantum well (QW) lasers. The goal of further work could be a direct experimental study of this issue, which, as far as we know, is currently missing.

2. THEORETICAL MODEL: RATE EQUATIONS

In this work, we carry out a linear analysis of the stability of two modes of generation and, accordingly, two branches of laser characteristics. We use a model based on the following three rate equations (for charge carriers in the waveguide region and in the QW, as well as for photons in the cavity):

$$\frac{\partial n^{OCL}}{\partial t} = \frac{j}{eb} + N_{QW}\frac{1}{b}\frac{n^{QW}}{\tau_{esc}} - N_{QW}\frac{v_{capt,0}}{b} \times (1-f_n)n^{OCL} - B_{3D}(n^{OCL})^2, \quad (2)$$

$$\frac{\partial n^{QW}}{\partial t} = v_{capt,0}(1-f_n)n^{OCL} - \frac{n^{QW}}{\tau_{esc}} - B_{2D}(n^{QW})^2 - c_g g^{max}(2f_n-1)n^{ph}, \quad (3)$$

$$\frac{\partial n^{ph}}{\partial t} = N_{QW}c_g g^{max}(2f_n-1)n^{ph} - c_g(\beta+\alpha_{int})n^{ph}. \quad (4)$$

The model of three rate equations assumes electron-hole symmetry (i.e., the sameness of all parameters and quantities related to electrons and holes). Taking electron-hole asymmetry into account would require the use of a system of five rate equations (for electrons and holes in the waveguide region and in the QW, as well as for photons in the cavity) and would introduce additional complications without significantly affecting the physical picture as a whole.

The physical quantities included in equations (2)–(4) and not introduced earlier are: n^{OCL}—concentration of free charge carriers in the waveguide region, j – pump (injection) current density, e—electron charge, n^{QW}—two-dimensional concentration of charge carriers in each quantum well (QW), N_{QW}—number of

QWs, B_{2D}—coefficient of spontaneous radiative recombination in a two-dimensional QW material [19, 34], c_g—group speed of light, n_{ph}—two-dimensional concentration of photons (number of photons per unit area of the stripe contact) of stimulated radiation in the laser cavity, $\beta = (1/L)\ln(1/R)$—cavity loss associated with the radiation yield through the mirror(s), L—cavity length, R—mirror reflectivity.

The internal optical loss coefficient α_{int}, which depends on the concentration of charge carriers n^{OCL} in the waveguide region and is included in equation (4), is given in the form

$$\alpha_{int} = \alpha_0 + \sigma_{int} n^{OCL}, \quad (5)$$

where α_0—constant component that includes "built-in" (independent of n^{OCL}) loss. The non-instantaneousness of carrier capture from the waveguide region into the low-dimensional active region leads to the dependence of the concentration n^{OCL} on the injection current [34–38, 41–45] and, thus, to the dependence of the internal loss α_{int} on the injection current.

The occupancy (filling factor) f_n of the lower edge of the size quantization subband in the QW by charge carriers is not an independent quantity and is expressed through the two-dimensional concentration of charge carriers n^{QW} in the QW as follows [23, 34]:

$$f_n = 1 - \exp\left(-\frac{n^{QW}}{N_c^{2D}}\right). \quad (6)$$

The thermal escape time τ_{esc} of charge carriers from the QW into the waveguide region is also not an independent quantity and is expressed through the velocity of capture $v_{capt,0}$ of charge carriers from the waveguide region into the unfilled QW as follows:

$$\tau_{esc} = \frac{1}{v_{capt,0}(1 - f_n)} \frac{N_c^{2D}}{n_1}. \quad (7)$$

In expressions (6) and (7), the quantity $N_c^{2D} = m_c^{QW} T/(\pi\hbar^2)$—two-dimensional effective density of states in the QW, m_c^{QW}—the effective mass of charge carriers in the QW, T—temperature in energy units.

The quantity n_1 in expression (7) is determined as follows [34]:

$$n_1 = N_c^{3D} \exp\left(-\frac{\Delta E_c - \varepsilon_n^{QW}}{T}\right), \quad (8)$$

where $N_c^{3D} = 2[(m_c^{OCL} T)/(2\pi\hbar^2)]^{3/2}$—three-dimensional effective density of states in the waveguide region, m_c^{OCL}—effective mass of charge carriers in the waveguide region, ΔE_c—QW depth for charge carriers (band offset at the heterointerface between the waveguide region and the QW), ε_n^{QW}—energy of the lower edge of the subband of size quantization of charge carriers in a QW.

3. ANALYSIS OF THE STABILITY OF MODES OF GENERATION

Within the framework of linear stability analysis, the solutions of rate equations (2)–(4) (time-dependent concentrations of charge carriers in the waveguide region (n^{OCL}) and in the QW (n^{QW}), as well as the concentration of photons (n^{ph}) in the resonator) are presented in the following form:

$$n^{OCL}(t) = n_0^{OCL} + (\delta n_m^{OCL})\exp(\Lambda t), \quad (9)$$

$$n^{QW}(t) = n_0^{QW} + (\delta n_m^{QW})\exp(\Lambda t), \quad (10)$$

$$n^{ph}(t) = n_0^{ph} + (\delta n_m^{ph})\exp(\Lambda t), \quad (11)$$

where n_0^{OCL}, n_0^{QW} and n_0^{ph} – solutions of the steady state rate equations, and δn_m^{OCL}, δn_m^{QW}, and δn_m^{ph}—small amplitudes of time-dependent components.

3.1. Steady-State Light-Current Characteristic

Solving the rate equations (2)–(4) at $\partial/\partial t = 0$ gives the steady-state values of the concentrations of free charge carriers in the waveguide region n_0^{OCL}, charge carriers localized in the QW, n_0^{QW}, as well as stimulated emission photons n_0^{ph} as functions of the pump current density j and parameters of the laser structure. Next, the steady-state output optical power of the laser $P_0 = \hbar\omega c_g \beta n_0^{ph} S$ is calculated, where $\hbar\omega$—photon energy, $S = WL$—stripe contact area, W—stripe contact width.

Here, as in works [41–45], an edge-emitting laser structure with a broadened waveguide is considered. The active region of the laser presents a single stressed QW. The materials of the QW, waveguide region and emitters (cladding layers) are $In_{0.31}Ga_{0.69}As$, GaAs and $Al_{0.1}Ga_{0.9}As$, respectively. The widths of the QW and waveguide region are 30 Å and 0.9 μm, respectively. The QW is not located in the center of the waveguide region, but closer to the p-emitter (at a distance of 0.1 μm from it). The concentrations of the majority charge carriers in the emitters $n_{clad} = p_{clad} = 5 \times 10^{18}$ cm^{-3}. The cross section of internal optical loss in the waveguide region $\sigma_{int} = 3 \times 10^{-18}$ cm^2; the velocity of capture of charge carriers from the waveguide region into an empty QW $v_{capt,0} = 10^6$ cm/s; length of the Fabry–Perot resonant cavity $L = 1.5$ mm, reflec-

tivities of both mirrors $R = 0.32$, width of the stripe contact $W = 100$ μm, temperature $T = 300$ K. The calculated maximum modal gain in a single QW $g^{\max} = 30.73$ cm^{-1}. The lasing wavelength is 0.98 μm.

For the structure under consideration, the quantity included in the left side of criterion (1) is equal to 2.65 and, thus, the rate equations have two solutions, which correspond to two modes of generation. The threshold current densities for the first and second modes $j_{\text{th, 1}} = 31.6$ A/cm^2 and $j_{\text{th, 2}} = 34$ kA/cm^2. The maximum pump current density, above which laser generation is disrupted, is $j^{\max} = 48.06$ kA/cm^2 (at this injection current density, the first and second branches of the LCC merge together—see Fig. 1).

Figure 1 shows the dependence of the output optical power on the injection current density (LCC) for the structure under consideration. As can be seen from the figure, the LCC consists of two branches. Above the first threshold, the first ("conventional") mode of generation is switched on, which corresponds to the first branch of the LCC (branch *1* in Fig. 1), above the second threshold, the second ("additional") mode of generation emerges, which corresponds to the second branch of LCC (branch *2* in Fig. 1). The generation in both branches is disrupted at the pump current density $j = j^{\max}$.

3.2. Characteristic Equation

For the existence of non-zero solutions for small amplitudes δn_m^{OCL}, δn_m^{QW} and δn_m^{ph} included in (9)–(11), the following characteristic equation (obtained by linearizing equations (2)–(4) using the expressions (9)–(11)) should be satisfied to find the eigenvalues Λ:

$$\Lambda^3 + A_2\Lambda^2 + A_1\Lambda + A_0 = 0, \tag{12}$$

where the expressions for the coefficients A_0, A_1 and A_2 are:

$$\begin{aligned} A_0 &= c_g g^{\max}(2f_{n0} - 1) \\ &\times \left\{ 2g^{\max}\left[N_{\text{QW}} \frac{v_{\text{capt,0}}}{b}(1 - f_{n0}) + 2B_{\text{3D}} n_0^{\text{OCL}} \right] \right. \\ &\left. - \frac{v_{\text{capt,0}}}{b}(n_1 + n_0^{\text{OCL}})\sigma_{\text{int}} \right\} N_{\text{QW}} \frac{1 - f_{n0}}{N_c^{\text{2D}}} c_g n_0^{\text{ph}}, \end{aligned} \tag{13}$$

$$\begin{aligned} A_1 &= N_{\text{QW}} \frac{v_{\text{capt,0}}}{b}(1 - f_{n0}) \\ &\times \left(2B_{\text{2D}} n_0^{\text{QW}} + 2c_g g^{\max} \frac{1 - f_{n0}}{N_c^{\text{2D}}} n_0^{\text{ph}} \right) \\ &+ 2B_{\text{3D}} n_0^{\text{OCL}} \left[v_{\text{capt,0}}(1 - f_{n0}) \frac{n_1 + n_0^{\text{OCL}}}{N_c^{\text{2D}}} \right. \\ &\left. + 2B_{\text{2D}} n_0^{\text{QW}} + 2c_g g^{\max} \frac{1 - f_{n0}}{N_c^{\text{2D}}} n_0^{\text{ph}} \right] \\ &+ c_g g^{\max}(2f_{n0} - 1)\left[2N_{\text{QW}} c_g g^{\max} \frac{1 - f_{n0}}{N_c^{\text{2D}}} n_0^{\text{ph}} \right], \end{aligned} \tag{14}$$

$$\begin{aligned} A_2 &= v_{\text{capt,0}}(1 - f_{n0})\left(\frac{N_{\text{QW}}}{b} + \frac{n_1 + n_0^{\text{0CL}}}{N_c^{\text{2D}}} \right) \\ &+ 2B_{\text{3D}} n_0^{\text{0CL}} + 2B_{\text{2D}} n_0^{\text{QW}} + 2c_g g^{\max} \frac{1 - f_{n0}}{N_c^{\text{2D}}} n_0^{\text{ph}}. \end{aligned} \tag{15}$$

The characteristic equation (12) is cubic since our model is based on three rate equations (see equations (2)–(4)).

Expressions (13)–(15) for the coefficients A_0, A_1 and A_2 include the steady-state values of the concentrations of charge carriers and photons n_0^{OCL}, n_0^{QW} and n_0^{ph}, which are the solutions to the system of rate equations (2)–(4) at $\partial/\partial t = 0$ and depend on the parameters of the laser structure and pump current density j. Therefore, the coefficients A_0, A_1 and A_2 also depend on j.

Since for the laser structure under consideration the rate equations have two solutions, each of the two modes of generation corresponds to its own values of the coefficients A_0, A_1 and A_2 and its eigenvalues Λ.

Within the framework of linear analysis, in order for the considered mode of generation to be stable, the exponential components in the expressions (9)–(11) should be evanescent (solutions (9)–(11) of the system of rate equations (2)–(4) should return over time to their steady-state values n_0^{OCL}, n_0^{QW} and n_0^{ph}), i.e. the real parts of all three eigenvalues Λ should be negative:

$$\text{Re}(\Lambda) < 0. \tag{16}$$

A positive sign of the real part of even one of the three eigenvalues Λ would mean an exponential increase in solutions (9)–(11), i.e., their departure from steady-state values and the instability of the mode of generation under consideration.

Thus, to determine the stability of modes of generation, it would suffice to determine the signs of the real parts of the roots of the cubic equation (12). Since the coefficients A_0, A_1 and A_2 in equation (12) are real quantities, there are the following two possibilities for the roots of equation (12) (eigenvalues Λ): (i) one real and a pair of complex conjugate roots; (ii) three real roots.

If all three coefficients A_0, A_1 and A_2 were always (at any pump current) positive, then, as can be seen from (12), the real eigenvalue(s) Λ would necessarily be negative, and the corresponding solutions would be stable. Since $f_{n0} < 1$ and all quantities included in expressions (14) and (15) for A_1 and A_2 are positive, the coefficients A_1 and A_2 are indeed always positive.

However, unlike A_1 and A_2, as can be seen from expression (13) for A_0, it is impossible a priori to draw any conclusion about the sign of the coefficient A_0. Thus, to even determine the stability of the solutions corresponding to the real eigenvalue(s), an analysis of at least the dependence of the sign of the coefficient A_0 on the injection current j is required. If it turns out that the coefficient A_0 is negative, then this will also not automatically lead to any conclusion about the sign of the real eigenvalue(s) Λ—since the coefficient A_2 is always positive, the second (quadratic) term on the left side of the equation (12) is always positive and formally the real eigenvalue(s) Λ can be both positive and negative. Thus, in the case of a negative coefficient A_0, to determine the sign of the real eigenvalue(s) Λ, the solution of equation (12) will be required.

It should be noted that since $2f_{n0} - 1 > 0$ (the condition for the positivity of the steady state population inversion and the gain coefficient in the active region—see [11]), as can be seen from (13), in the absence of internal optical loss that depends on the concentration of charge carriers in the waveguide region (i.e., at $\sigma_{int} = 0$), the coefficient A_0 is also always positive. Thus, in this case the real eigenvalue(s) Λ are negative. This result reflects the fact that in the absence of internal loss, which depends on the concentration of charge carriers in the waveguide region, there is only one solution to the system of rate equations and, accordingly, only one ("conventional") mode of generation, which is always stable.

In Subsection 3.2.1 we analyze the coefficients A_0, A_1 and A_2. Since no conclusion can be made about the sign of the real part of the complex-conjugate eigenvalues even in the case of all positive coefficients A_0, A_1 and A_2, and it turns out that the coefficient A_0 is negative for the second mode of generation, then further (in Section 3.2.2) we solve equation (12) to find the eigenvalues Λ.

3.2.1. Coefficients A_0, A_1 and A_2 of the characteristic equation as functions of the pump current density. Having calculated the steady state concentrations n_0^{OCL}, n_0^{QW} and n_0^{ph} for each of the modes of generation and using further formulas (13)–(15), we determined the coefficients A_0, A_1 and A_2 for two branches. Figure 2 shows these coefficients as functions of the pump current density. As can be seen from the figure, the coefficients A_0, A_1 and A_2 for the first mode of generation (curves *1*) are always positive. For the second mode of generation, the coefficients A_1 and A_2 (curves *2*) are also always positive, but the coefficient A_0 for the laser structure under study is always negative. At the laser emission cut-off point ($j = j^{max}$), the coefficients A_0, A_1 and A_2 for the two modes (as well as all other characteristics for them) coincide.

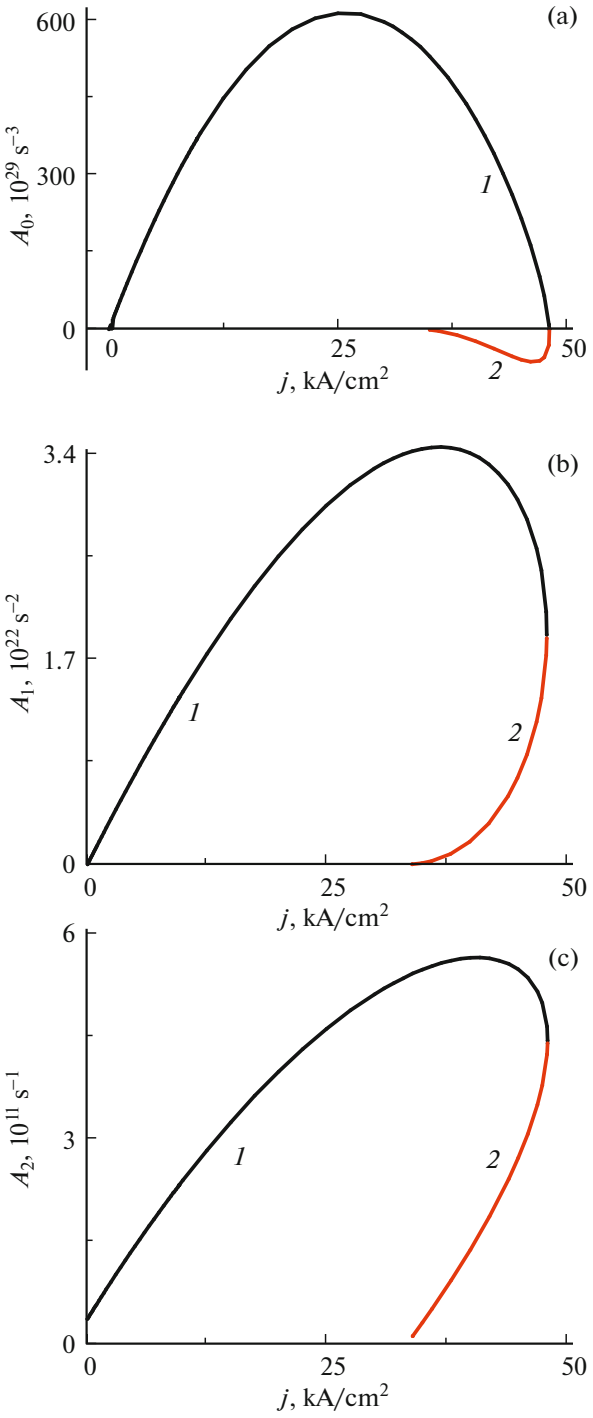

Fig. 2. Coefficients A_0, A_1 and A_2 of the characteristic equation (12) against pump current density. *1* – first mode of generation, *2* – second mode of generation.

3.2.2. Roots Λ_1, Λ_2 and Λ_3 of the characteristic equation as functions of the pump current density. Having calculated the coefficients A_0, A_1 and A_2, we then find the roots Λ of the cubic equation (12) for each of the two modes of generation (Figs. 3–6).

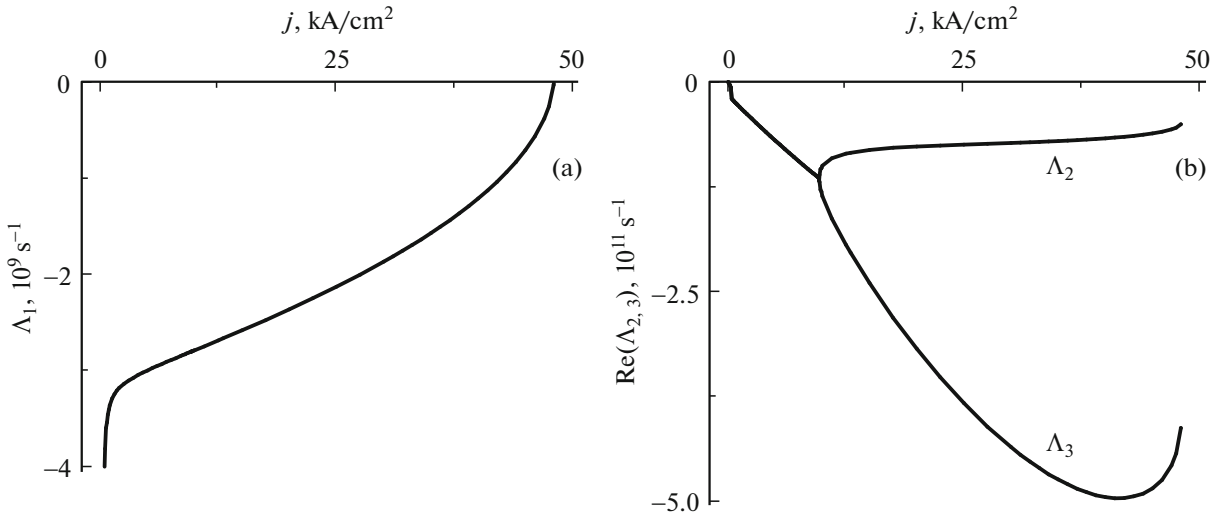

Fig. 3. Real eigenvalue Λ_1 (a) and real parts of eigenvalues Λ_2 and Λ_3 (b) for the first ("conventional") mode of generation against pump current density.

Let us start with an analysis of the roots for the first ("conventional") mode of generation. As can be seen from Fig. 3a, one of the eigenvalues (Λ_1) for the first mode of generation is always (for all values of the pump current, i.e., for $j_{th,\,1} < j < j^{max}$) a real negative quantity. It turned out that the other two roots (Λ_2 and Λ_3) for the first mode of generation are complex conjugate quantities at pump current densities in the range $j_{th,\,1} < j < 9.6$ kA/cm^2. The real part of these roots is also negative (Fig. 3b). The imaginary parts of the roots Λ_2 and Λ_3, which are equal in magnitude but opposite in sign, are shown in Fig, 4. Solutions in the form (9)–(11), corresponding to the roots Λ_2 and Λ_3 at pump currents in the range $j_{th,\,1} < j < 9.6$ kA/cm^2, describe underdamped relaxation oscillations in the laser—the absolute value of the imaginary parts of the roots Λ_2 and Λ_3 is the angular frequency of these oscillations (see [46, 47]).

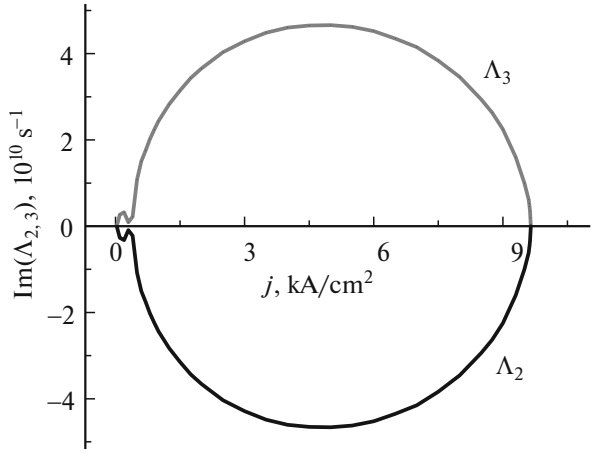

Fig. 4. Imaginary parts of the eigenvalues Λ_2 and Λ_3 for the first ("conventional") mode of generation against pump current density.

As can be seen from Fig. 4, at $j = 9.64$ kA/cm^2, the imaginary parts of the roots Λ_2 and Λ_3 (i.e., the angular frequency of relaxation oscillations) go to zero (compare with Fig. 2 in [46, 47]). (In Fig. 4 we should also note a peculiarity in the dependence of Im(Λ_2) and Im (Λ_3) on the pump current density at values of j slightly exceeding $j_{th,\,1}$.)

As can be seen from Fig. 3b, at $j > 9.64$ kA/cm^2, the roots Λ_2 and Λ_3 become purely real (while differing from each other) negative quantities. Solutions in the form (9)–(11) at pump currents $j > 9.64$ kA/cm^2 describe overdamping, i.e. purely exponentially evanescent (without oscillations) relaxation of the concentrations of charge carriers and photons to their steady state values.

Thus, as can be seen from our calculations, for the first ("conventional") mode of generation, the real parts of the eigenvalues (or real eigenvalues) of all three roots Λ are negative in the entire range of operating currents in the laser $j_{th,1} < j < j^{max}$ (Fig. 3). This proves the stability of the first mode of generation: the second terms on the right side of expressions (9)–(11) decay exponentially in time, and, thus, the concentrations of charge carriers and photons return to their steady state values n_0^{OCL}, n_0^{QW} and n_0^{ph}.

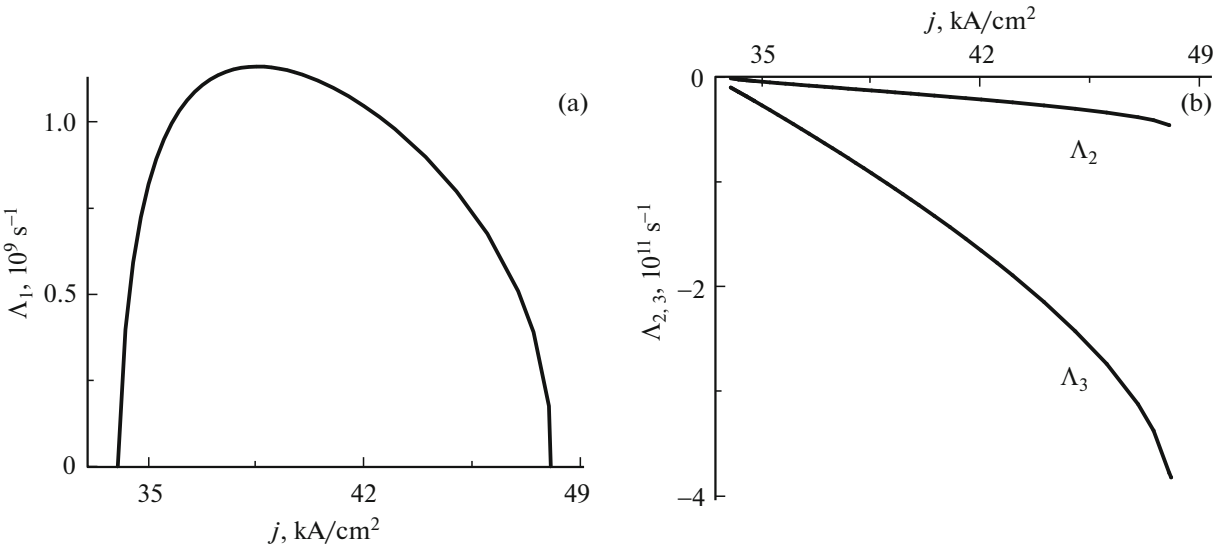

Fig. 5. Real eigenvalues Λ for the second ("additional") mode of generation against pump current density: (a) positive root Λ_1; (b) negative roots Λ_2 and Λ_3.

Let us proceed to the analysis of the roots of the characteristic equation (12) for the second ("additional") mode of generation as functions of the pump current density. These roots are shown in Fig. 5. It turned out that all three roots are real quantities: one root (Λ_1) is always (for all values of the pump current for the second mode of generation, i.e., for $j_{th,2} < j < j^{max}$) positive (Fig. 5a), and the other two (Λ_2 and Λ_3) are always negative (Fig. 5b).

Figures 6a–6c shows the real parts of the roots Λ_1, Λ_2 and Λ_3 for two modes of generation ("conventional" and "additional") as functions of the pump current density. It can be seen from the figure that at the lasing cut-off point (at $j = j^{max}$) the corresponding eigenvalues for the two modes coincide. This, in particular, means that the roots Λ_1 for two modes of generation (which have opposite signs for $j < j^{max}$) should necessarily vanish at this point (Fig. 6a).

Thus, our calculations show that for the second mode of generation the eigenvalue Λ_1 is positive over the entire range of pump currents ($j_{th,2} < j < j^{max}$). This proves the instability of the second mode of generation in the considered laser structure: the second terms on the right side of expressions (9)–(11), corresponding to this root Λ_1, increase exponentially in time and, thus, the concentrations of charge carriers and photons move away from their steady state values n_0^{OCL}, n_0^{QW} and n_0^{ph}.

4. CONCLUSIONS

A linear analysis of the stability of two modes of generation in semiconductor quantum well lasers has been carried out. Two modes of generation correspond to two solutions to the system of rate equations, obtained taking into account the internal optical loss that depends on the concentration of charge carriers in the waveguide region of the laser. It is shown that, in contrast to the always stable and, therefore, observable first ("conventional") mode of generation, the second ("additional") mode, which is entirely due to the carrier-concentration-dependent internal loss, is unstable and, therefore, cannot be observed under steady state conditions in the considered laser structure.

Despite the fact that the second mode of generation is unstable and cannot be observed under steady state conditions, i.e., with a constant pump current (continuous wave operation), its existence can manifest itself under pulsed pumping at current densities $j > j_{th,2}$. Even possible short-term switches from the stable first ("conventional") mode to the unstable second should be accompanied by a strong increase in the intensity of radiation associated with the spontaneous recombination of charge carriers (in the waveguide region in the first place, but also in the quantum well) and, accordingly, a drop in the useful power of stimulated radiation from the quantum well (see Fig. 1). Thus, fluctuations of spontaneous and stimulated emissions under pulsed pumping can serve as indica-

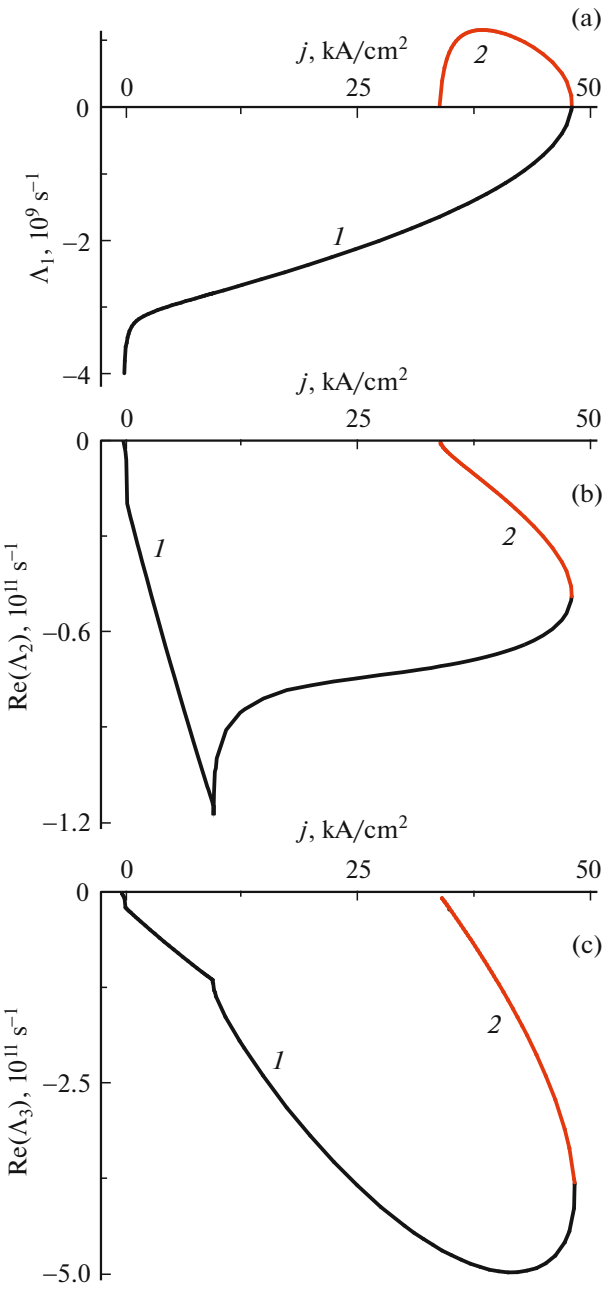

Fig. 6. Real eigenvalue Λ_1 (a) and real parts of the eigenvalues Λ_2 (b) and Λ_3 (c) against pump current density. *1* – first ("conventional") mode of generation, *2* – second ("additional") mode of generation.

tors of the existence of an unstable second mode of generation.

FUNDING

The work of Z.N. Sokolova has been performed under state assignment of Ioffe Institute of Physics and Technology.

CONFLICT OF INTEREST

The authors declare that they have no conflict of interest.

REFERENCES

1. Zh. I. Alferov, V. M. Andreev, D. Z. Garbuzov, Yu. V. Zhilyaev, E. P. Morozov, E. L. Portnoi, V. G. Trofim. Sov. Phys. Semicond., **4**, 1573 (1970).
2. R. Dingle, C. H. Henry. U.S. Patent no. 3982207 (1976).
3. R. D. Dupuis, P. D. Dapkus, N. Holonyak, E. A. Rezek, R. Chin. Appl. Phys. Lett., **32**, 295 (1978).
4. W. T. Tsang. Appl. Phys. Lett., **40**, 217 (1982).
5. P. G. Yeliseyev. *Vvedeniye v fiziku inzhektsionnykh lazerov* (M., Nauka, 1983). (in Russian).
6. Zh. I. Alferov, D. Z. Garbuzov, A. V. Ovchinnikov, I. S. Tarasov, V. P. Evtikhiev, A. B. Nivin, A. E. Svelokuzov. Pis'ma ZhTF, **11**, 1157 (1985). (in Russian).
7. Zh. I. Alferov, A. I. Vasil'ev, S. V. Ivanov, P. S. Kop'ev, N. N. Ledentsov, M. E. Lutsenko, B. Ya. Mel'tser, V. M. Ustinov. Sov. Techn. Phys. Lett., **14**, 782 (1988).
8. D. Z. Garbuzov, A. V. Ovchinnikov, N. A. Pikhtin, Z. N. Sokolova, I. S. Tarasov, V. B. Khalfin. Sov. Phys. Semicond., **25**, 560 (1991).
9. *Quantum Well Lasers,* ed. by P. S. Zory, jr. (Academic, Boston, 1993).
10. A. Y. Egorov, A. E. Zhukov, P. S. Kop'ev, N. N. Ledentsov, M. V. Maksimov, V. M. Ustinov. Semiconductors, **28**, 809 (1994).
11. L. V. Asryan, R. A. Suris. Semicond. Sci. Technol., **11** (4), 554 (1996).
12. L. J. Mawst, A. Bhattacharya, J. Lopez, D. Botez, D. Z. Garbuzov, L. DeMarco, J. C. Connolly, M. Jansen, F. Fang, R. F. Nabiev. Appl. Phys. Lett., **69**, 1532 (1996).
13. R. F. Kazarinov, G. E. Shtengel. J. Lightwave Technol., **15**, 2284 (1996).
14. *Semiconductor Lasers,* ed. by E. Kapon (Academic, San Diego, 1999).
15. L. V. Asryan, N. A. Gun'ko, A. S. Polkovnikov, G. G. Zegrya, R. A. Suris, P.-K. Lau, T. Makino. Semicond. Sci. Technol., **15** (12), 1131 (2000).
16. Zh. I. Alferov. Rev. Mod. Phys., **73**, 767 (2001).
17. H. Kroemer. Rev. Mod. Phys., **73**, 783 (2001).
18. L. V. Asryan, R. A. Suris. Semiconductors, **38** (1), 1 (2004).
19. L. V. Asryan. Quant. Electron., **35** (12), 1117 (2005).
20. V. V. Bezotosnyi, V. V. Vasil'eva, D. A. Vinokurov, V. A. Kapitonov, O. N. Krokhin, A. Yu. Leshko, A. V. Lyutetskii, A. V. Murashova, T. A. Nalet, D. N. Nikolaev, N. A. Pikhtin, Yu. M. Popov, S. O. Slipchenko, A. L. Stankevich, N. V. Fetisova, V. V. Shamakhov, I. S. Tarasov. Semiconductors, **42**, 350 (2008).
21. D.-S. Han, L. V. Asryan. Appl. Phys. Lett., **92** (25), 251113 (2008).
22. S. L. Chuang. *Physics of Photonic Devices,* 2nd ed (New York, NY, USA: Wiley, 2009).

23. L. V. Asryan, N. V. Kryzhanovskaya, M. V. Maximov, A. Yu. Egorov, A. E. Zhukov. Semicond. Sci. Technol., **26** (5), 055025 (2011).
24. M. T. Crowley, N. A. Naderi, H. Su, F. Grillot, L. F. Lester. Semicond. Semimet., **86**, 371 (2012). (San Diego, CA, USA: Elsevier). https://doi.org/10.1016/B978-0-12-391066-0.00010-1
25. C. Wang, B. Lingnau, K. Ludge, J. Even, F. Grillot. IEEE J. Quant. Electron., **50**, 723 (2014).
26. K. Nishi, K. Takemasa, M. Sugawara, Y. Arakawa. IEEE J. Select. Top. Quant. Electron., **23**, 1901007 (2017).
27. V. Mikhelashvili, O. Eyal, I. Khanonkin, S. Banyoudeh, V. Sichkovskyi, J. P. Reithmaier, G. Eisenstein. J. Appl. Phys., **124**, 054501 (2018).
28. A. E. Zhukov, A. M. Nadtochiy, N. V. Kryzhanovskaya, Yu. M. Shernyakov, N. Yu. Gordeev, A. A. Serin, S. A. Mintairov, N. A. Kalyuzhny, A. S. Payusov, G. O. Kornyshov, M. V. Maksimov, Y. Wang. FTP, **56** (9), 922 (2022). (in Russian).
29. E. Alkhazraji, W. W. Chow, F. Grillot, J. E. Bowers, Y. Wan. Light: Sci. Appl., **12**, 162 (2023).
30. L. V. Asryan, S. Luryi. Appl. Phys. Lett., **83** (26), 5368 (2003).
31. L. V. Asryan, S. Luryi. IEEE J. Quant. Electron., **40** (7), 833 (2004).
32. L. V. Asryan. Appl. Phys. Lett., **88** (7), 073107 (2006).
33. L. V. Asryan. J. Nanophoton., **3**, 031601 (2009).
34. Z. N. Sokolova, I. S. Tarasov, L. V. Asryan. Semiconductors, **45** (11), 1494 (2011).
35. L. V. Asryan, S. Luryi, R. A. Suris. Appl. Phys. Lett., **81** (12), 2154 (2002).
36. L. V. Asryan, S. Luryi, R. A. Suris. IEEE J. Quant. Electron., **39** (3), 404 (2003).
37. L. V. Asryan, Z. N. Sokolova. J. Appl. Phys., **115** (2), 023107 (2014).
38. Z. N. Sokolova, N. A. Pikhtin, I. S. Tarasov, L. V. Asryan. J. Phys.: Conf. Ser., **740**, 012002 (2016). https://doi.org/10.1088/1742-6596/740/1/012002
39. L. Jiang, L. V. Asryan. IEEE Photon. Technol. Lett., **18** (24), 2611 (2006).
40. Y. Wu, L. Jiang, L. V. Asryan. J. Appl. Phys., **118** (18), 183107 (2014).
41. Z. N. Sokolova, N. A. Pikhtin, L. V. Asryan. J. Lightwave Technol., **36** (11), 2295 (2018). https://doi.org/10.1109/JLT.2018.2806942
42. Z. N. Sokolova, N. A. Pikhtin, L. V. Asryan. *Proc. 18th Int. Conf. on Laser Optics "ICLO 2018"* (St. Petersburg, Russia, June 4–8, 2018. Paper no. ThR3-p31, p. 169).
43. Z. N. Sokolova, N. A. Pikhtin, L. V. Asryan. Electron. Lett., **55** (9), 550 (2019). https://doi.org/10.1049/el.2019.0225
44. Z. N. Sokolova, N. A. Pikhtin, S. O. Slipchenko, L. V. Asryan. Proc. SPIE, **11301**, 113010D (2020). (Novel In-Plane Semiconductor Lasers XIX 2020; San Francisco, USA; February 3–6, 2020). https://doi.org/10.1117/12.2546974
45. Z. N. Sokolova, N. A. Pikhtin, S. O. Slipchenko, L. V. Asryan. 8th Int. School and Conf. "Saint Petersburg Open 2021" on Optoelectronics, Photonics, Engineering and Nanostructures, SPb OPEN 2021. J. Phys.: Conf. Ser., **2086**, 012076 (2021). https://doi.org/10.1088/1742-6596/2086/1/012076
46. L. V. Asryan, R. A. Suris. Appl. Phys. Lett., **96** (22), 221112 (2010).
47. L. V. Asryan, R. A. Suris. Proc. SPIE, **7610**, 76100R (2010).

Translated by E. Potapova